Article

Nanoengineered concrete with coloidal sílica for repair of concrete structures

Concreto nanoestruturado com sílica coloidal para reparo de estruturas de concreto

Abstract

Pathological manifestations in concrete structures result from failures in design, execution, maintenance, or material degradation, thus requiring effective repair solutions towards extending the structures' service life. Nanoengineered concrete with colloidal silica can be an efficient alternative as a repair material, for it reduces porosity and increases mechanical strength due to its effect on the interfacial transition zone between the aggregate and the cement paste. This study evaluates the application of a high-strength concrete with colloidal silica as a repair material to conventional concrete structural elements. Cylindrical and prismatic concrete specimens were produced, intentionally damaged, and subsequently repaired with the developed special concrete. Characterization results revealed significant improvement in the mechanical properties of the special concrete even at low colloidal silica contents, being the best compressive strength obtained with the addition of only 1% colloidal silica, by cement mass. The repaired elements showed satisfactory performance in all measured properties, maintaining compressive strength values statistically similar to those of intact conventional concrete after 28 days of repair (39.4 MPa and 40.7 MPa for repaired and intact specimens, respectively). The results highlight the potential of nanoengineered concrete with colloidal silica addition for practical structural repair applications.

Keywords: Special concrete. Repair material. Colloidal silica. Nanotechnology.

Resumo

Manifestações patológicas em estruturas de concreto resultam de falhas no projeto, execução, manutenção ou degradação do material, exigindo soluções eficazes de reparo para prolongar sua vida útil. O concreto nanoestruturado com sílica coloidal pode ser uma alternativa eficiente como material de reparo, pois essa adição promove redução da porosidade e aumento da resistência mecânica, devido à sua atuação na zona de transição entre o agregado e a pasta de cimento. Este estudo avalia a aplicação de concreto de alta resistência com adição de sílica coloidal como material de reparo em elementos estruturais de concreto convencional. Para isso, foram produzidos corpos de prova cilíndricos e prismáticos de concreto convencional, posteriormente danificados e reparados com o concreto especial desenvolvido. Os resultados de caracterização revelaram uma melhora significativa nas propriedades mecânicas do concreto especial mesmo com baixos teores de sílica coloidal, sendo a melhor resistência à compressão obtida com a adição de apenas 1% de sílica coloidal, em relação à massa de cimento. Os elementos reparados apresentaram desempenho satisfatório em todas as propriedades avaliadas, mantendo valores de resistência à compressão estatisticamente semelhantes aos do concreto convencional intacto após 28 dias do reparo (39,4 MPa e 40,7 MPa para os elementos reparados e intactos, respectivamente). Os resultados obtidos demonstram o potencial do concreto nanoestruturado com sílica coloidal em aplicações práticas de reparo estrutural.

Palavras-chave: *Concretos especiais. Material de reparo. Sílica coloidal. Nanotecnologia.*

[1]Lucas Modotte Bernardo
[1]Universidade de São Paulo
São Carlos - SP - Brasil
lucasmodottebernardo@gmail.com

[2]*Alessandra Lorenzetti de Castro
[2]Universidade de São Paulo
São Carlos - SP - Brasil
alcastro@sc.usp.br

Recebido em 04/08/25
Revisado em 19/12/25
Aceito em 23/12/25

*corresponding author

1 Introduction

Several problems have arisen in structures concomitantly with the intense use of Portland cement concrete, since designing a concrete structure goes beyond the application of structural engineering concepts. The characteristics and the behavior of the constituent materials and the significant interference of the environment to which the structure will be exposed must be taken into account for ensuring the durability of the structure (ABNT, 2023). However, ensuring the durability of concrete structures is a challenge for the construction industry, as various internal and external mechanisms cause the material to age and deteriorate, which is aggravated by poor preventive maintenance, as well as inadequate construction practices.

An effective treatment of pathologies in concrete structures requires identifying the main causes and extent of deterioration and selecting appropriate repair strategies. According to Santos (2019), based on NBR 6118 (ABNT, 2023), degradation mechanisms affect the concrete (leaching, sulfate expansion, alkali-aggregate reaction), the reinforcement (corrosion induced by carbonation and chloride ions), and the structure itself (mechanical/cyclic actions, thermal movements, impact, shrinkage, creep, relaxation, among other actions on the structure). Despite good practices in design, construction, use, and maintenance, these mechanisms often compromise durability, and Brazilian standardization for recovery and repair remains limited. However, there are international technical codes such as ACI 562-25 (ACI, 2025) that establish minimum requirements for the assessment of damage and deterioration, and for the design of repair and rehabilitation strategies for existing structural concrete buildings (ACI, 2025).

Maintenance can be preventive or corrective. The former is characterized by measures taken in advance and foreseen during the use and maintenance of the structure, whereas the latter corresponds to diagnosis, prognosis, repair, and protection of structures that already show pathological manifestations. Corrective actions include recovery (restoring minimum performance), reinforcement (increasing load-bearing capacity), and repair (achieving the minimum performance predicted by design). Furthermore, the post-rehabilitation performance depends on the overall compatibility between substrate and repair material. This compatibility involves not only mechanical strength but also dimensional stability (such as shrinkage and thermal deformation) and stiffness, which must be consistent with the type of repair and the structural purpose of the intervention. In some applications, materials more resistant than the original concrete, such as grout, structural mortars, or even metallic reinforcement are used, whereas in other situations more deformable repair materials may be appropriate. In all cases, the repair material must ensure effective bond and low degradability, as it is applied to critical regions of the structure. When assessing materials for use in concrete repair, tests that simulate stress states representative of service conditions are recommended, which include direct tensile bond strength, flexural tensile strength, direct shear, and flexural shear tests (Fagury, 2002).

In this context, special concretes containing chemical admixtures and mineral additions have emerged towards solving pathological manifestations and guaranteeing greater durability of structures. Among such concretes and with the advance of nanoscience associated with concrete technology, those with addition of colloidal silica stand out. This nano-addition with rounded particles produces an "ultra-filler" effect (Norhasri *et al.*, 2017) and, due to the larger surface area, ensures greater pozzolanic activity (Li *et al.*, 2017). Thus, the nanoparticles can act as nucleation points for cement phases, promoting greater hydration due to their high reactivity, as nano reinforcement, and as a filler material, densifying the microstructure and the transition zone, thus reducing the porosity of the concrete (Rupasinghe *et al.*, 2011). Therefore, concrete with colloidal silica shows low permeability and high compressive strength from the earliest age, properties that indicate it as a possible candidate to fulfill that repair function in structures. As an example, the material can be used for rapid structural repairs on bridges that cannot remain long closed and usually face problems such as concrete spalling, concreting failures, and reinforcement exposure (Medeiros *et al.*, 2020).

Colloidal silica, a key nanomaterial in cement-based systems, consists of amorphous silicon dioxide nanoparticles (nano-SiO_2) stabilized in aqueous suspension, produced by controlled polymerization of $Si(OH)_4$ molecules from silicic acid in chemical reactors (Magliano, 2009). Its particle size ranges from 2 to 20 nm, with specific surface areas between 300 and 900 m²/g. The nano-addition acts as a rheology-modifying agent and enhances early mechanical strength, since it destabilizes in the presence of soluble cationic chemical species, initiating a gelation reaction and forming C-S-H nano-seeds that accelerate cement hydration. It produces both a pozzolanic activity and a filler effect in the concrete matrix (Singh *et al.*, 2013), which are very important effects in developing special concretes such as high and ultra-high performance ones.

However, the ideal colloidal silica content to be added to the concrete mixture remains uncertain, as studies report divergent results regarding its effects on water demand to maintain workability in the fresh state (Ltifi *et al.*, 2011; Quercia *et al.*, 2012; Zhang *et al.*, 2014; Supit; Shaikh, 2015; Yun *et al.*, 2022) and on compressive strength in the hardened state (Bjormstrom *et al.*, 2004; Li *et al.*, 2004; Qing *et al.*, 2007; Jo *et al.*, 2007; Salemi; Behfarnia, 2013; Zhang *et al.*, 2014; Kong *et al.*, 2019; Yun *et al.*, 2022). As for durability, reported benefits include substantial reductions in chloride penetration and decreased capillary water absorption, confirming its suitability for aggressive environments (Said *et al.*, 2012; Jalal *et al.*, 2015; Kong *et al.*, 2019; Santos, 2019).

Although previous studies have suggested that concrete with colloidal silica presents promising characteristics for use as a repair material, the direct assessment of its performance when applied to deteriorated conventional concrete elements remains limited. Addressing this gap, the present study evaluates the use of nanoengineered concrete with colloidal silica as a repair material in conventional concrete elements, analyzing the properties of the special concrete in both fresh and hardened states and its effectiveness in restoring damaged elements.

2 Materials and methods

2.1 Characterization of the constituent materials

Portland cement, fine and coarse aggregates, water, silica fume, quartz powder, limestone filler, superplasticizer admixture, and colloidal silica were used for the production of conventional and special concretes.

2.1.1 Portland cement

Slag-modified Portland cement of 32 MPa strength class (CPII E 32) was used in the conventional concrete mixture, for it is widely employed in current concrete structures. High-early strength Portland cement (CPV ARI) was used in the special, high-strength concrete mixtures because its rapid strength development at early ages allows for faster demolding and handling of repaired elements after curing. The same consideration was made by Vaske *et al.* (2008), who investigated the strengthening of concrete columns with silica fume mortar and also selected CPV ARI to ensure early strength gain and expedite the demolding process, thus improving the efficiency of the repair technique. The specific gravity of the cements was in accordance with NBR 16605 (ABNT, 2017a) and the particle size distribution was determined by laser particle size analysis, in accordance with ISO 13320 (ISO, 2020), using the FRITSCH ANALYSETTE 22 NanoTec equipment. The chemical analysis of the cements was performed by X-ray fluorescence (XRF).

2.1.2 Fine aggregate

Two natural quartz sands, classified as fine and medium sands, were used. An industrialized natural sand, commercially known as AG 80-100, was employed particularly for the special concrete mixture. Each material was characterized separately; density and water absorption were determined according to NBR 16916 (ABNT, 2021a) and granulometric composition was established according to NBR 17054 (ABNT, 2022).

2.1.3 Coarse aggregate

Basaltic crushed stone of 19 mm maximum size and commercially classified as “crushed stone 1” was used for conventional concrete mixture, whereas crushed stone of same origin, but of 9.5 mm maximum size and commercially classified as “crushed stone 0” was employed for special concrete mixture. Density and water absorption of both aggregates were determined according to NBR 16917 (ABNT, 2021b) and granulometric composition was defined according to NBR 17054 (ABNT, 2022).

2.1.4 Mixing water

Water from the local water supply was used. According to NBR 15900-1 (ABNT, 2009), this water is considered suitable for use in concrete and does not need to be tested.

2.1.5 Silica fume

Silica fume was used only for the production of the special concrete mixtures. Specific gravity was determined according to NBR 16605 (ABNT, 2017a), laser particle size distribution was based on ISO 13320 (ISO, 2020), specific surface area was established by Blaine method, prescribed in NBR 16372 (ABNT, 2015a), and chemical analysis was performed by X-ray fluorescence (XRF).

2.1.6 Quartz powder

Quartz powder, commercially known as SM200, was added only to the special concrete mixtures. For characterization purposes, the same characterization tests applied to silica fume were conducted.

2.1.7 Limestone filler

Limestone filler was also used only in special concrete mixtures. Specific gravity was determined according to NBR 16605 (ABNT, 2017a), laser particle size distribution was based on ISO 13320 (ISO, 2020), and chemical analysis was performed by X-ray fluorescence (XRF).

2.1.8 Superplasticizer admixture

A polycarboxylate-based superplasticizer admixture (ADVA 458 UHPC, manufactured by Chryso Saint-Gobain) was added during the production of the mixtures to ensure the desired consistency for the concretes would be met.

2.1.9 Colloidal silica

A single type of colloidal silica, i.e., an aqueous dispersion of nanosilica with an approximately 50% solids concentration was used. Therefore, the water constituting the colloidal silica was deducted from the mixing water to maintaining the water/cement ratio established for each mixture. Chemical analysis by X-ray fluorescence (XRF) was also performed.

2.2 Preparation of conventional concrete specimens for repair

2.2.1 Mix design and validation of the conventional concrete mixture

Since the characteristics of the conventional concrete specimens should be similar to those typical of current concrete structures built in Brazilian construction industry, a concrete mixture was designed by IPT/EPUSP method (Helene; Terzian, 1992), targeting a compressive strength (f_{ck}) of 35 MPa and slump of (120 ± 20) mm.

The mixture was validated through tests in both fresh and hardened states. In the fresh state, slump was measured following NBR 16889 (ABNT, 2020), and specific gravity and air content were determined by the gravimetric method, according to NBR 9833 (ABNT, 2008). In the hardened state, the compressive strength was determined following NBR 5739 (ABNT, 2018a), at 7 and 28 days, testing three cylindrical specimens of 100 mm in diameter and 200 mm in height, at each age.

2.2.2 Preparation of specimens for repair

After validation of the conventional concrete mixture, cylindrical and prismatic specimens were molded to allow analysis under compression and flexural tensile stresses, respectively. The cylindrical specimens were 100 mm in diameter and 200 mm in height, whereas the prismatic specimens were 150 mm x 150 mm x 500 mm, both molding according to NBR 5738 (ABNT, 2015b). After demolding, all conventional concrete specimens were kept in wet curing until the respective mechanical test ages.

After 28 days of curing, specimens destinated for damage and subsequently repaired were kept in the laboratory environment for a pre-conditioning stage until reaching constant mass, ensuring they would be "dry" at the moment of damage and repair. The repaired specimens were returned to wet curing for an additional 28 days before the tests to evaluate the repair performance.

2.2.3 Damage to the specimens

Prismatic specimens were damaged by the four-point flexural tensile strength test, according to NBR 12142 (ABNT, 2010). The test typically causes failure near mid-span, producing an irregular surface, conducive to the adhesion of the repair material (Figures 1a and 1b).

Figure 1 – **Specimen surfaces ready for application of the repair material: (a) prismatic specimen after four-point bending test; (b) prismatic specimen irregular surface; and (c) cylindrical specimen surface after manual roughening**

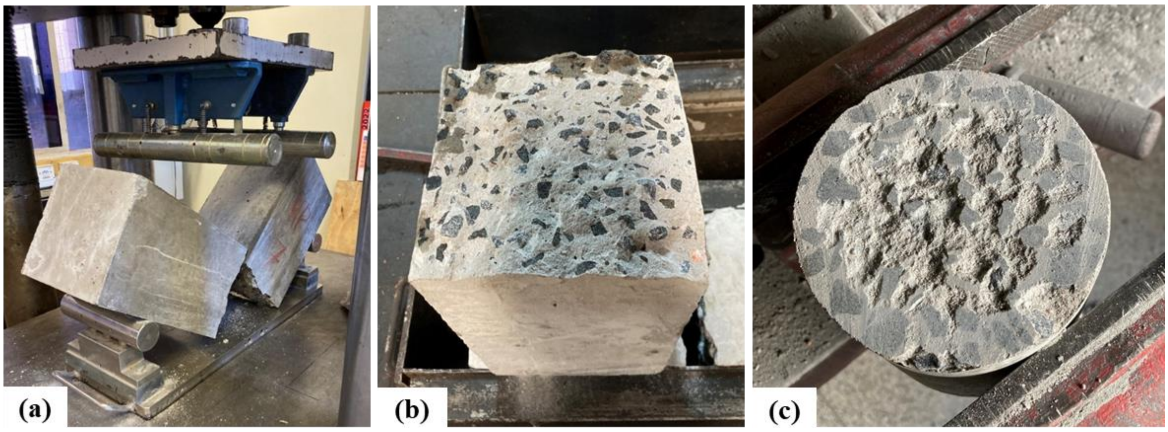

Cylindrical specimens were sawn transversely at mid-height, forming two smaller cylinders of approximately 100 mm in diameter and 100 mm in height and smooth surfaces after cutting. Similarly to the procedure performed by Vaske *et al.* (2008), the sawn surface was manually roughened using hammer and chisel to create surface texture and expose coarse aggregates (Figure 1c). This procedure enables a better adhesion of the repair material, improving the performance of the interface between the conventional concrete specimen and the binding material (Prado, 2020).

After damage, the surfaces were cleaned with compressed air and brushing to remove loose particles and dust. No bonding agents or surface treatments were applied before casting the repair concrete.

2.3 Development of the nanoengineered concrete with colloidal silica

2.3.1 Mix design and selection of ideal colloidal silica content

The mix design of the special concrete with colloidal silica addition was based on the particle packing concept and Alfred's model, which defines a continuous particle size distribution aimed at maximizing packing density and minimizing voids within the granular structure. In addition to its simplicity regarding the mathematical formulation, such model considers the maximum and minimum particle size limits and improves the concrete efficiency (Funk; Dinger, 1994). The method was integrated with the computational optimization procedure proposed by Lopes (2019):

by implementing Alfred's model in spreadsheets, the theoretical concrete curve is plotted, indicating the distribution that minimizes void content; then, through an iterative optimization process aimed at maximizing the correlation coefficient (R^2) between the experimental and theoretical curves, the composition of the experimental mixture is determined, setting the distribution coefficient according to the desired workability of the concrete. Thus, in the present study, the particle size curves of the selected constituent granular materials were input into the mathematical model to generate a theoretical curve, later adjusted to experimental results. A high-strength concrete mixture was obtained from this computational optimization, targeting a compressive strength (f_{ck}) above 80 MPa.

After designing this base mixture, concretes were produced with the addition of colloidal silica at contents of 1%, 2.5%, 5%, and 10%, by cement mass. Two parameters guided the selection of the ideal colloidal silica content: the mixture spread in the fresh state, set at (230 ± 30) mm, and the compressive strength at 7 and 28 days, testing three cylindrical specimens of 100 mm in diameter and 200 mm in height, at each age.

2.3.2 Characterization of the special concrete

Once the high-strength concrete mixture and the ideal colloidal silica content were defined, the repair material, i.e., nanoengineered concrete with colloidal silica, was characterized. The tests listed in Table 1 were performed, with three specimens tested at each age for all physical and mechanical evaluations in the hardened state.

Table 1 – **Tests for characterizing the special concrete**

Tests	Reference standards	Specimens	Test ages (days)
Setting time in cement paste	NBR 16607 (ABNT, 2018b)	---	---
Spread (slump flow)	NBR 15823-2 (ABNT, 2017b)	---	---
Specific gravity in fresh state	NBR 9833 (ABNT, 2008)	---	---
Compressive strength	NBR 5739 (ABNT, 2018a)	Cylindrical (∅ 100 mm x 200 mm)	7 and 28
Specific gravity, water absorption by immersion and void ratio	NBR 9778 (ABNT, 2005a)	Cylindrical (∅ 100 mm x 200 mm)	28
Tension strength in flexure	NBR 13279 (ABNT, 2005b)	Prismatic (40 mm x 40 mm x 160 mm)	28
Static modulus of elasticity by compression	NBR 8522-1 (ABNT, 2021c)	Cylindrical (∅ 100 mm x 200 mm)	28
Dynamic modulus of elasticity	NBR 8522-2 (ABNT, 2021d)	Prismatic (40 mm x 40 mm x 160 mm)	7 and 28
Ultrasonic wave transmission velocity	NBR 8802 (ABNT, 2019)	Prismatic (40 mm x 40 mm x 160 mm)	2, 7 and 28

2.4 Repair of the damaged elements and analysis of the repair performed

The final stage consisted of repairing the damaged elements using the developed and characterized special concrete and evaluating the effectiveness of the repair. The repair process occurred 150 days after the production of the conventional concrete specimens. The repair material acted as a bond between the two parts of the specimens, i.e., cylindrical and prismatic ones, which were split in half, forming a layer of repair material of 1 to 2 cm thick. The tests in Table 2 were considered in the evaluation of the repair performance. The experiments began at the first ages of the conventional concrete specimens and continued until 178 days after their production, corresponding to 28 days after the repair. For each test age, three specimens were evaluated.

3 Results and discussion

3.1 Characterization of the constituent materials

The results of the characterization tests of the constituent materials are summarized in Tables 3 and 4. Figure 2 graphically shows the discrete particle size distribution of the granular materials, i.e., percentage of material retained in each sieve.

The granular materials chosen tend to fill different particle size ranges, which is essential for achieving a higher packing density in concrete mixtures (Oliveira *et al.*, 2018). The increasing order of particle size starts with colloidal silica, silica fume, CPV ARI, CPII E 32, quartz powder (SM200), and limestone filler and ends with industrial sand (AG 80-100), fine sand, medium sand, "crushed stone 0", and "crushed stone 1" aggregates, respectively. The colloidal silica fit into the region with particles between 0.01 and 0.10 µm diameter, reiterating its "ultra-filler" effect (Norhasri *et al.*, 2017), since the nanomaterial filled the voids even between the silica fume particles (0.10 to 10 µm), as shown in the particle size curves in Figure 2.

Table 2 – **Tests for evaluating the repair performed**

Tests	Reference standards	Specimens	Test ages (days)	
			Conventional concrete	**Repaired specimens**
Compressive strength	NBR 5739 (ABNT, 2018a)	Cylindrical (∅ 100 mm x 200 mm)	7, 28, 150, 178	157, 178
Tension strength in flexure	NBR 12142 (ABNT, 2010)	Prismatic (150 mm x 150 mm x 500 mm)	28, 150	178
Static modulus of elasticity by compression	NBR 8522-1 (ABNT, 2021c)	Cylindrical (∅ 100 mm x 200 mm)	28, 178	178
Dynamic modulus of elasticity	NBR 8522-2 (ABNT, 2021c)	Cylindrical (∅ 100 mm x 200 mm)	7, 28, 150, 178	157, 178
Ultrasonic wave transmission velocity	NBR 8802 (ABNT, 2019)	Cylindrical (∅ 100 mm x 200 mm)	7, 28, 150, 178	152, 157, 178

Table 3 – **Chemical analysis results from X-ray fluorescence (XRF)**

Compounds (%)	CPII E 32	CPV ARI	AG 80-100	Silica fume	SM200	Limestone filler	Colloidal silica
SiO_2	21.83	16.44	99.74	98.63	99.80	2.60	99.57
Al_2O_3	5.51	3.29	---	---	---	0.43	---
Fe_2O_3	3.06	4.21	0.15	---	---	0.39	---
CaO	64.80	68.96	0.11	0.25	0.09	95.67	0.21
SO_3	2.09	4.33	---	0.33	0.11	---	---
K_2O	0.26	0.39	---	0.58	---	---	---
TiO_2	0.52	0.29	---	---	---	---	---
MnO	0.46	0.14	---	---	---	---	---

Table 4 – **Results of physical characterization tests on the constituent materials**

	Material	**Specific gravity (g/cm³)**	**Water absorption (%)**	**Maximum size (mm)**	**Fineness modulus**
Aggregates	“Crushed stone 1”	2.82	0.33	19.00	3.61
	“Crushed stone 0”	2.99	0.53	9.50	5.84
	Medium sand	2.56	0.63	1.18	1.16
	Fine sand	2.59	0.15	4.75	2.37
Industrial aggregate	Material	Specific gravity (g/cm³)	d_{50} (µm)		
	AG 80-100	2.64	150		
Binders	Material	Specific gravity (g/cm³)	d_{50} (µm)		
	CP II E 32	2.95	13.40		
	CPV ARI	3.16	9.29		
Mineral addition	Material	Specific gravity (g/cm³)	d_{50} (µm)		Surface area - Blaine (cm²/g)
	Silica fume	2.20	1.40		17900
	SM200	2.70	31.80		2340
	Limestone filler	2.60	13.40		-
Chemical admixture	Material	Specific gravity (g/cm³)	Description		Appearance
	ADVA 458 UHPC	1.075 – 1.115	Polycarboxylate-based superplasticizer		Orange liquid
Nanomaterial	Material	Specific gravity (g/cm³)	Solids content		Appearance
	Colloidal silica	1.40	50%		White liquid

Figure 2 - **Discrete particle size distribution curves of the granular constituent materials**

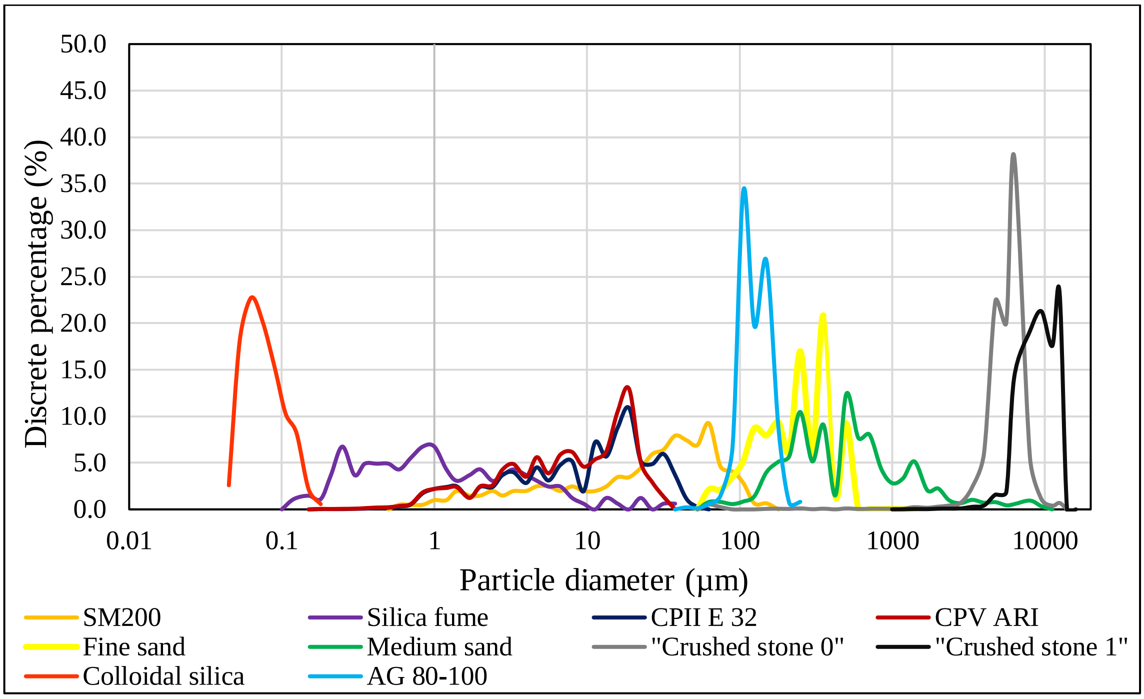

3.2 Preparation of conventional concrete specimens for repair

The conventional concrete composition and the results of the validation tests conducted in fresh and hardened states are shown in Table 5. The results were considered satisfactory, since the slump and compressive strength values initially established were obtained from the conventional concrete mix design. Therefore, after validation of the conventional concrete mixture, the specimens for repair were molded. After the specimens had cured, part of them was damaged for later repair.

3.3 Development of the nanoengineered concrete with colloidal silica

3.3.1 Mix design and selection of ideal colloidal silica content for special concretes

The composition of the special reference concrete (CI-REF), without the addition of colloidal silica, is presented in Table 6. New mixtures were produced based on that concrete mix design and considering the addition of different colloidal silica contents, so that their influence on the behavior of the mixtures in the fresh state can be observed in Table 6. The results of the compressive strength test of all the mixtures produced are presented graphically in Figure 3.

According to the results, maintaining the predetermined spread of (230 ± 30) mm, the increase in the amount of colloidal silica resulted in a greater demand for superplasticizer admixture. Supit and Shaikh (2015) and Ltifi *et al.* (2011) observed similar relationships. Supit and Shaikh (2015) reported a 40% and 60% reduction in slump with the addition of 2% and 4% colloidal silica, respectively, whereas Ltifi *et al.* (2011) claimed the addition of 3% colloidal silica in relation to the cement mass required incorporation of more water for maintaining the workability of the cement-based mixtures.

In the hardened state, compressive strength increased 8.5% at 28 days with the addition of 1.0% colloidal silica (a significant difference) and 5.8% with the addition of 2.5%. Mechanical strength reduced at 28 days for both mixtures at the two highest contents (5% and 10%). The improvement in mechanical performance of "CI-1%" mixture can be compared to the results of Qing *et al.* (2007) and Zhang *et al.* (2014), who also used a 1% colloidal silica addition and obtained, respectively, 20% and 4% increases in compressive strength in comparison to the reference mixtures. The low compressive strength values for mixtures with high colloidal silica contents can be explained by the difficulty in obtaining the correct dispersion of large amounts of that addition. Bjormstrom *et al.* (2004) observed a similar behavior, reporting a reduction in the mechanical performance of concrete with colloidal silica content greater than 2%.

Table 5 – **Composition and tests results of conventional concrete**

Mix design, by mass	Cement	Fine sand	Medium sand	"Crushed stone 1"	Water
	1.00	0.78	1.16	2.61	0.47
Material consumption (kg/m³ of concrete)					
Cement (CPII E 32)	411				
Fine sand	319				
Medium sand	478				
"Crushed stone 1"	1072				
Water	193				
Characterization tests					
Slump value	130 mm				
Specific gravity	2.47 g/cm³				
Air content	2.3%				
Compressive strength – 7 days	f_{cm} = 24.83 MPa (SD = 0.06 MPa / CV = 0.25%)				
Compressive strength – 28 days	f_{cm} = 38.77 MPa (SD = 1.43 MPa / CV = 3.70%)				

Note: f_{cm} = mean compressive strength; SD = standard deviation; and CV = coefficient of variation

Table 6 – **Compositions and test results for each colloidal silica content**

Mixture	Reference high-strength concrete (CI-REF)				
Mix design, by mass	Cement	Silica fume	Quartz powder	AG 80-100	Water
	1.00	0.21	0.25	1.10	0.20
Material consumption (kg/m³ of concrete)	Cement	870			
	Silica fume	183			
	SM 200	217			
	AG 80-100	957			
	Water	174			
Behavior in fresh state					
Mixture identification	CI-REF	CI-1%	CI-2.5%	CI-5%	CI-10%
Superplasticizer (% of cement mass)	2.50%	2.75%	3.00%	3.75%	5.00%
Spread value (mm)	235	235	230	205	165

Figure 3 – **Compressive strength results for each colloidal silica content**

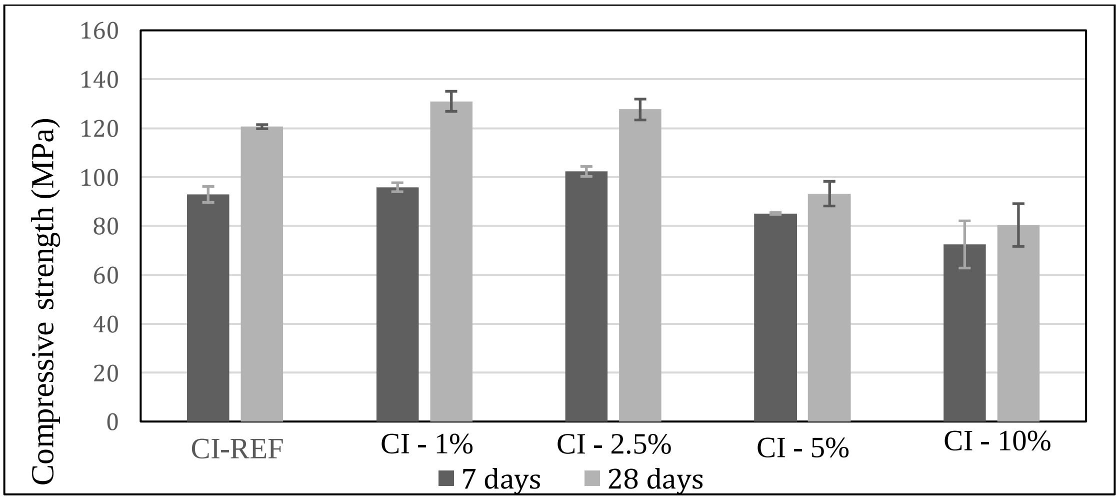

Therefore, according to the results in Table 6 and Figure 3, the colloidal silica content to be used in special concrete for repair would be 1% per mass of cement, which is justified economically (lower costs for the superplasticizer admixture and colloidal silica itself) and mechanically. However, the initial special concrete mixture resulted in a compressive strength value much higher than the initially specified (f_{ck} of 80 MPa), characterizing it as an ultra-high performance concrete, as it reached 120 MPa compressive strength at 28 days. This mechanical behavior may differ from that observed in commercially available repair materials, which, despite having high compressive strength, typically do not exceed 60 MPa at 28 days of age. Furthermore, the resulting mixture increases the costs associated with the constituent materials and can hinder practical application due to its consistency, especially in the repair of small and medium-sized works. Therefore, an adjustment was made to the mixture in order to obtain a material with mechanical performance close to that available on the market, but colloidal silica addition was kept at 1% per mass of cement.

The final composition of the special concrete (CE-1%) and the results of the tests for the validation of its behavior in fresh and hardened states are shown in Table 7. The results from the adjusted and final mixture met the expected parameters, since the reference mixture (CE-REF) reached 80.23 MPa compressive strength at 28 days. Moreover, the compressive strength of the concrete with colloidal silica (CE-1%) increased 10.6% in comparison to the reference and, therefore, was the special concrete composition characterized and used as a repair material.

3.3.2 Characterization of the special concrete

Characterization tests were conducted on the special concrete with colloidal silica (see Table 8 for the results). From this point onwards, the special concrete containing 1% colloidal silica will be referred to as “CE-1%" and the only material used in the structural repair of the subsequent stages.

Table 7 – **Final composition and test results for the special concrete**

Mix design, by mass	Cement	Silica fume	Limestone filler	Fine sand	Medium sand	“Crushed stone 0”	Water
	1.00	0.10	0.30	0.29	0.43	0.72	0.19

Material consumption (kg/m³ of concrete)	
Cement	792
Silica fume	79
Limestone filler	238
Fine sand	288
Medium sand	342
“Crushed stone 0”	570
Water	151

Mixture	Superplasticizer (% of cement mass)	Spread value (mm)	7 days			28 days		
			f_{cm} (MPa)	SD (MPa)	CV (%)	f_{cm} (MPa)	SD (MPa)	CV (%)
CE-REF	2.20%	250	68.92	1.70	2.46	80.23	3.66	4.56
CE-1%	2.50%	245	68.98	1.96	2.85	88.72	1.80	2.03

Note: fcm = mean compressive strength; SD = standard deviation; CV = coefficient of variation

Table 8 – **Characterization of the special concrete with colloidal silica (CE-1%)**

Test	Results	Unit
Specific gravity in the fresh state	2.49 ± 0.06	g/cm³
Water absorption by immersion	1.69 ± 0.01	%
Void ratio	3.47 ± 0.03	%
Specific gravity in the hardened state	2.53 ± 0.03	g/cm³
Tension strength in flexure at 28 days	13.05 ± 0.03	MPa
Static modulus of elasticity at 28 days	48.5 ± 1.17	GPa
Dynamic modulus of elasticity at 7 days	51.6 ± 1.48	GPa
Dynamic modulus of elasticity at 28 days	54.4 ± 1.13	GPa
Ultrasonic wave transmission velocity (2 days)	4632.05 ± 60.62	m/s
Ultrasonic wave transmission velocity (7 days)	5143.53 ± 40.62	m/s
Ultrasonic wave transmission velocity (28 days)	5281.23 ± 14.66	m/s

Among the results of the characterization tests, the low void ratio recorded stands out, showing the influence of colloidal silica on the mixture, i.e., mitigating the porosity of the composite through its "ultra-filler" effect and high pozzolanic activity (Li *et al.*, 2017). The results are in agreement with those reported by Du *et al.* (2015), who observed densification of the cement paste microstructure and reduction of the transition zone even with the addition of low contents of colloidal silica (0.3% to 0.9% per cement mass).

Regarding modulus of elasticity, according to Metha and Monteiro (2014), the dynamic modulus of elasticity values for high-strength concrete are approximately 20% higher than the static modulus of elasticity. In the present study, a comparison of dynamic and static modulus of elasticity values obtained at 28 days showed a 12.2% difference for CE-1%.

The ultrasonic wave transmission velocity was measured in prismatic specimens under the saturated surface-dry condition, at three ages, namely, 2, 7, and 28 days. Velocity was measured in the longitudinal direction of the prisms for analyses of a wider range of the material. Naik, Malhotra and Popovics (2004) classified the quality of concrete according to the ultrasonic wave transmission velocity, such that velocities of 5000 m/s, 4000 m/s, and 3000 m/s are related to concrete mixtures classified as very good, medium, and very poor quality, respectively. On the seventh day after molding, CE-1% reached velocity values greater than 5000 m/s, indicating very good quality for the mixture produced.

The setting time test was conducted separately from the other characterization tests. Vicat apparatus measured the setting time of the cement paste, following the guidelines of NBR 16607 (ABNT, 2018b). Adopting the water/cement ratio of the concrete mixture, two cement pastes were produced, namely, one with no colloidal silica and another with 1% of the nanomaterial in relation to the cement mass. The initial and final setting times obtained for both cement pastes are shown in Table 9.

The data in Table 9 indicate an acceleration in the initial and final setting times due to the addition of colloidal silica to the cement paste. A decrease of more than 4 hours (240 minutes) in setting times was observed between the two mixtures and can be understood as a direct response to the complex interaction between colloidal silica and cement. As discussed by Singh *et al.* (2013) and Magliano (2009), colloidal silica acts as a rheology-modifying agent in concrete and an enhancer of its mechanical strength in the earliest ages. That is due to its ability to destabilize in presence of soluble cationic chemical species, triggering a gelation reaction that results in the formation of additional C-S-H nano-seeds, thus accelerating cement hydration and, consequently, reducing the setting times of the mixture.

3.4 Repair of the damaged elements and analysis of the repair performed

This section presents the results of conventional concrete specimens from their earliest ages until their repair with special concrete containing colloidal silica. The specimens repaired with CE-1% were designated "Repaired CE-1%." Tests on the repaired cylinders (Figure 4a) determined compressive strength, static and dynamic modulus of elasticity, and ultrasonic wave transmission velocity, at 7 and 28 days after repair. The repaired prisms (Figure 4b) were tested only for four-point flexural tensile strength.

3.4.1 Compression and flexural tensile strengths

Towards a good comparison between the reference results (intact conventional concrete specimens) and those of the repaired specimens, the evolution of the compressive strength was monitored from the earliest ages up to 28 days after the repair, which corresponds to 178 days. The results from the compressive strength test are illustrated graphically in Figure 5. Those of the mechanical tests are satisfactory, since the compressive strength of the repaired specimens was close to the strength value of the reference sample (intact specimens) 28 days after the repair, with no statistically significant differences (Bernardo, 2024). A widespread cracking of the specimen was observed at failure in all tests (Figure 6a); however, no displacement of the repair material occurred.

Table 9 – **Characterization of special concrete: cement paste setting times**

Parameter	CE-REF	CE-1%
Initial setting time (min)	520	266
Final setting time (min)	610	336

Figure 4 - **Specimens repaired with nanoengineered concrete with colloidal silica**

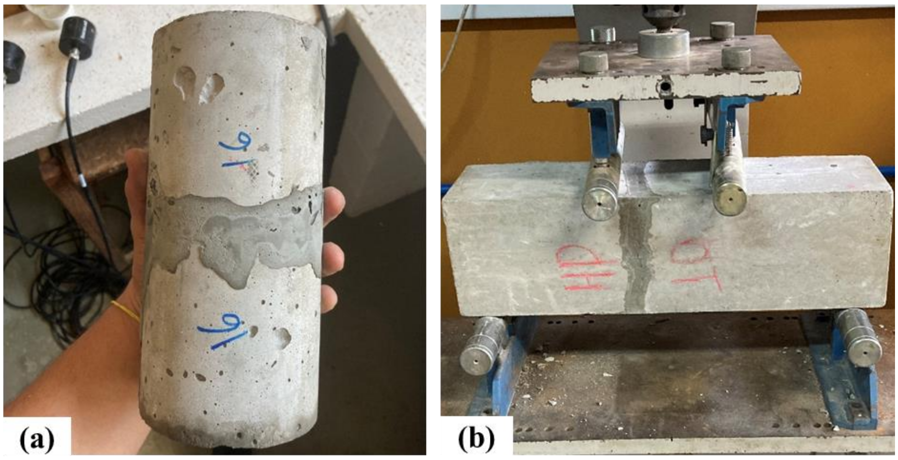

Figure 5 - **Analysis of the repair with special concrete: evolution of compressive strength**

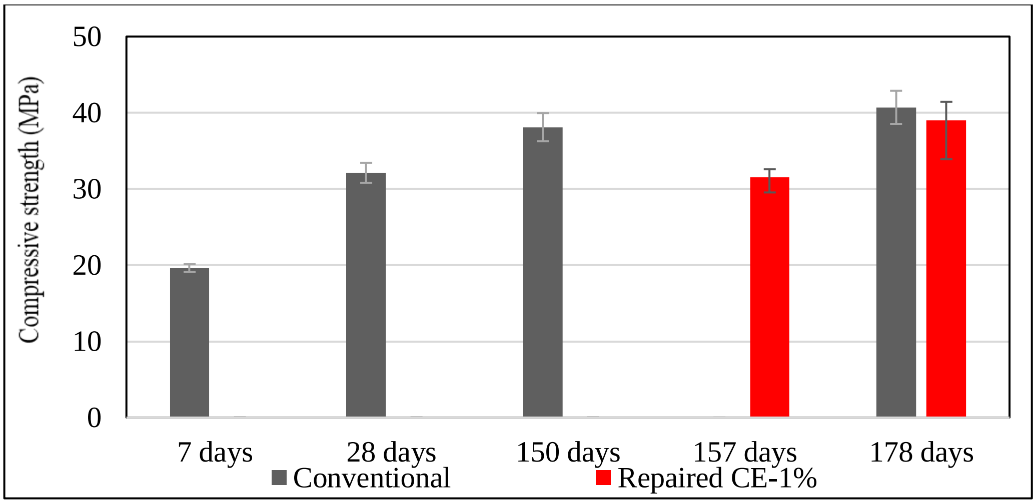

Figure 6 - **Repaired specimens subjected to mechanical (destructive) tests**

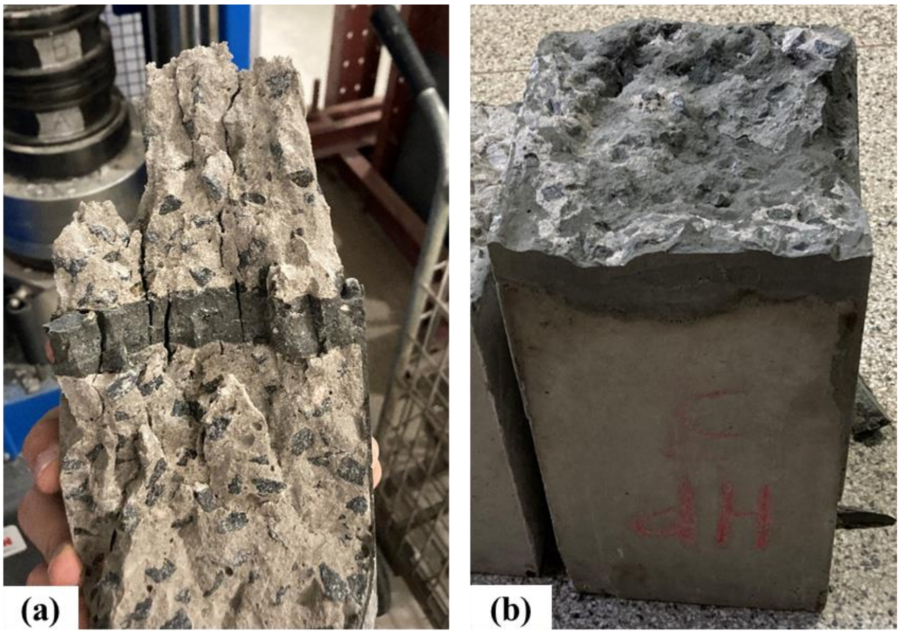

Table 10 shows the results from the evaluation of intact and repaired specimens through the flexural tensile test. A significant difference in flexural tensile strength is observed when comparing the values obtained from intact and repaired specimens (Bernardo, 2024), with an 8.5% reduction in the flexural tensile strength of the repaired specimens in comparison to the values obtained from intact conventional concrete specimens, when considering the results obtained at the age of 150 days for the intact specimens and at the of 178 days for the repaired specimens, i.e., 28 days after repair.

Since no bonding material was applied between the conventional concrete and the repair concrete, the interface between those materials became the element's weakest point for flexural stress. Although all repaired specimens failed upon contact, there were traces of both concretes on the failure surfaces (Figure 6b), demonstrating the bonding of the repair material to the "old" concrete of the specimen even with no application of adhesives or Portland cement pastes to the surface to be repaired. Performing the same test method and using Portland cement paste as a bonding bridge between old concrete and repair concrete, Fagury (2002) observed the repaired prismatic specimen failed in the old concrete and, in some cases, reached a higher strength value in comparison to the intact specimen. However, the author obtained flexural tensile strength values ranging between 3 and 4 MPa with mixtures similar to those developed in this study and results comparable to the present ones.

3.4.2 Modulus of elasticity

The modulus of elasticity was measured by both static by compression and dynamic tests (see Tables 11 and 12, respectively, for the results). The static modulus of elasticity values of repaired specimens (Repaired CE-1%) were similar to those of the intact specimens (Conventional), which highlights the effectiveness of the repair with the special concrete with colloidal silica and suggests the modulus of elasticity was maintained at levels comparable to those of intact concrete even after separation and repair of the specimens. Such results reinforce the potential feasibility of using special concrete with colloidal silica for restoring the structural integrity of concrete elements.

According to Mehta and Monteiro (2014), the dynamic modulus of elasticity values for medium and low strength concretes are approximately 30% and 40% higher than those of the static modulus of elasticity, respectively. As shown in Tables 11 and 12, the differences between longitudinal dynamic modulus of elasticity (EL) and static modulus of elasticity obtained 28 days after the repair were 25.2% and 24.9% for the intact specimens and those repaired with special concrete, respectively. These correlations indicate that homogeneous and dense samples were obtained, and that the presence of the repair did not interfere with the elastic behavior of the material, indicating adequate adhesion between the substrate and the repair material and, therefore, the good quality of the service performed.

4.4.3 Ultrasonic wave transmission velocity

Ultrasonic wave transmission velocity was measured in the longitudinal direction of the cylindrical specimens and the results are shown in Table 13. The velocities recorded 28 days after the specimens had been repaired (178 days) were greater than 4500 m/s, indicating the quality of the concrete constituting the specimens can generally be classified as medium to very good (Naik; Malhotra; Popovics, 2004).

Table 10 – **Analysis of the repair with special concrete: flexural tensile strength results**

Age (days)	Identification	Conventional	Repaired CE-1%
28	$f_{ct,f,m}$ (MPa)	4.40	---
	SD (MPa)	0.01	---
	CV (%)	0.22	---
150 (REPAIR)	$f_{ct,f,m}$ (MPa)	5.01	---
	SD (MPa)	0.35	---
	CV (%)	7.08	---
178	$f_{ct,f,m}$ (MPa)	---	3.95
	SD (MPa)	---	0.09
	CV (%)	---	2.15

Note: $f_{ct,f,m}$ = mean flexural tensile strength; SD = standard deviation; and CV = coefficient of variation.

Table 11 – **Analysis of the repair with special concrete: static modulus of elasticity results**

Identification	Age (days)					
	28			178		
	$E_{ci,m}$ (GPa)	SD (GPa)	CV (%)	$E_{ci,m}$ (GPa)	SD (GPa)	CV (%)
Conventional	32.3	1.72	5.26	35.0	1.65	4.72
Repaired CE-1%	-	-	-	33.1	0.89	2.69

Note: $E_{ci,m}$ = mean value of static modulus of elasticity; SD = standard deviation; and CV = coefficient of variation.

Table 12 – **Analysis of the repair with special concrete: dynamic modulus of elasticity results**

Identification	Parameters	Age (days)				
		7	28	150	157	178
Conventional	EL (GPa)	37.0	42.8	43.0	-	43.8
	SD (GPa)	0.41	1.66	1.38	-	0.01
	CV (%)	1.11	3.87	3.21	-	0.02
	EF (GPa)	37.0	41.9	42.7	-	43.6
	SD (GPa)	1.74	1.28	1.44	-	0.01
	CV (%)	4.70	3.06	3.37	-	0.02
Repaired CE-1%	EL (GPa)	-	-	-	38.1	41.3
	SD (GPa)	-	-	-	0.61	0.01
	CV (%)	-	-	-	1.61	0.03
	EF (GPa)	-	-	-	37.7	42.7
	SD (GPa)	-	-	-	0.93	0.06
	CV (%)	-	-	-	2.46	0.15

Note: EL = mean value of longitudinal dynamic modulus of elasticity; EF = mean value of flexural dynamic modulus of elasticity; SD = standard deviation; and CV = coefficient of variation.

Table 13 – **Analysis of the repair with special concrete: ultrasonic wave transmission velocity results**

Age (days)		7	28	150	152	157	178
Conventional	VPU (m/s)	4441.47	4681.50	4756.37	-	-	4782.33
	SD (m/s)	18.22	6.22	51.79	-	-	45.38
	CV (%)	0.41	0.13	1.09	-	-	0.95
Repaired CE-1%	VPU (m/s)	-	-	-	4575.90	4631.63	4840.73
	SD (m/s)	-	-	-	33.16	35.94	16.56
	CV (%)	-	-	-	0.72	0.78	0.34

Note: VPU = mean value of the velocity; SD = standard deviation; and CV = coefficient of variation.

The increase in ultrasonic wave transmission velocity due to the replacement of part of the conventional concrete specimen with higher-strength and lower-porosity concrete was expected; however, the contact region between the materials may contain voids, which would reduce ultrasonic wave transmission velocity. An analysis of the data from the last reading revealed the velocities measured for the specimens repaired with CE-1% concrete were slightly higher than those measured for the reference (intact) specimens. Despite expectations of a possible significant difference due to the change to materials, no substantial distinction was observed among the results at 178 days of analysis.

4 Conclusions

The following conclusions were based on the experimental development and analyses conducted and their results:

(a) the use of colloidal silica in concrete significantly improved its mechanical performance, especially at lower addition contents. The 1% addition in relation to the cement mass increased compressive strength at 28 days, whereas additions of more than 2.5% reduced it;

(b) higher colloidal silica contents required a greater amount of superplasticizer to maintain workability, due to the difficulty in ensuring adequate dispersion of the silica nanoparticles;

(c) water absorption and void ratio confirmed colloidal silica significantly reduces concrete porosity, indicating its efficiency in producing denser and potentially more durable concretes;

(d) colloidal silica also acted as a rheology-modifying agent in cement pastes, reducing setting time by approximately 40% with the addition of 1% of the nanomaterial;

(e) specimens repaired with the special concrete containing 1% colloidal silica showed satisfactory mechanical performance. Compressive strength values exceeded 35 MPa and ultrasonic wave transmission velocity was higher than 4,700 m/s, confirming the high quality of the repair;

(f) the modulus of elasticity measured in the repaired specimens remained in the same order of magnitude of the intact specimens, demonstrating the mechanical compatibility between the repair material and the original conventional concrete; and

(g) the bonds between the "old" conventional concrete and the special repair concrete showed good adhesion, even with no use of adhesives or pastes as a bonding bridge. The presence of traces of both concretes on the failure surfaces of the repaired specimens confirmed the bonding potential of the special concrete with colloidal silica.

As a limitation of this study, the experimental program was conducted on reduced-scale specimens, which may not fully reproduce the behavior of structural elements in service. Future research could investigate the performance of the nanoengineered concrete with colloidal silica for repair larger elements and under conditions closer to real structural demands. Additionally, evaluating the cost implications and comparing the practical and economic performance of this repair solution with other materials commercially available would provide valuable insights for its broader application.

References

AMERICAN CONCRETE INSTITUTE. **ACI CODE 562-25**: assessment, repair and rehabilitation of existing concrete structures: code requirements and commentary. Farmington Hills, 2025.

ASSOCIAÇÃO BRASILEIRA DE NORMAS TÉCNICAS. **NBR 12142**: concreto: determinação da resistência à tração na flexão de corpos de prova prismáticos. Rio de Janeiro, 2010.

ASSOCIAÇÃO BRASILEIRA DE NORMAS TÉCNICAS. **NBR 13279**: argamassa de assentamento e revestimento de paredes e tetos: determinação da resistência à tração na flexão e à compressão. Rio de Janeiro, 2005b.

ASSOCIAÇÃO BRASILEIRA DE NORMAS TÉCNICAS. **NBR 15823-2**: concreto autoadensável: parte 2: determinação do espalhamento, do tempo de escoamento e do índice de estabilidade visual: método do cone de Abrams. Rio de Janeiro, 201b7.

ASSOCIAÇÃO BRASILEIRA DE NORMAS TÉCNICAS. **NBR 15900-1**: água para amassamento do concreto: parte 1: requisitos. Rio de Janeiro, 2009.

ASSOCIAÇÃO BRASILEIRA DE NORMAS TÉCNICAS. **NBR 16372**: cimento Portland e outros materiais em pó: determinação da finura pelo método de permeabilidade ao ar (método de Blaine). Rio de Janeiro, 2015a.

ASSOCIAÇÃO BRASILEIRA DE NORMAS TÉCNICAS. **NBR 16605**: cimento Portland e outros materiais em pó: determinação da massa específica. Rio de Janeiro, 2017a.

ASSOCIAÇÃO BRASILEIRA DE NORMAS TÉCNICAS. **NBR 16607**: cimento Portland: determinação do tempo de pega. Rio de Janeiro, 2018b.

ASSOCIAÇÃO BRASILEIRA DE NORMAS TÉCNICAS. **NBR 16889**: concreto: determinação da consistência pelo abatimento do tronco de cone. Rio de Janeiro, 2020.

ASSOCIAÇÃO BRASILEIRA DE NORMAS TÉCNICAS. **NBR 16916**: agregado miúdo: determinação da densidade e da absorção de água. Rio de Janeiro, 2021a.

ASSOCIAÇÃO BRASILEIRA DE NORMAS TÉCNICAS. **NBR 16917**: agregado graúdo: determinação da densidade e da absorção de água. Rio de Janeiro, 2021a.

ASSOCIAÇÃO BRASILEIRA DE NORMAS TÉCNICAS. **NBR 17054**: agregados: determinação da composição granulométrica: método de ensaio. Rio de Janeiro, 2022.

ASSOCIAÇÃO BRASILEIRA DE NORMAS TÉCNICAS. **NBR 5738**: concreto: procedimento para moldagem e cura de corpos de prova. Rio de Janeiro, 2015b.

ASSOCIAÇÃO BRASILEIRA DE NORMAS TÉCNICAS. **NBR 5739**: concreto: ensaio de compressão de corpos de prova cilíndricos. Rio de Janeiro, 2018a.

ASSOCIAÇÃO BRASILEIRA DE NORMAS TÉCNICAS. **NBR 6118**: projeto de estruturas de concreto. Rio de Janeiro, 2023.

ASSOCIAÇÃO BRASILEIRA DE NORMAS TÉCNICAS. **NBR 8522-1**: concreto endurecido: determinação dos módulos de elasticidade e de deformação: parte 1: módulos estáticos à compressão. Rio de Janeiro, 2021c.

ASSOCIAÇÃO BRASILEIRA DE NORMAS TÉCNICAS. **NBR 8522-2**: concreto endurecido: determinação dos módulos de elasticidade e de deformação: parte 2: módulo de elasticidade dinâmico pelo método das frequências naturais de vibração. Rio de Janeiro, 2021d.

ASSOCIAÇÃO BRASILEIRA DE NORMAS TÉCNICAS. **NBR 8802**: concreto endurecido: determinação da velocidade de propagação de onda ultrassônica. Rio de Janeiro, 2019.

ASSOCIAÇÃO BRASILEIRA DE NORMAS TÉCNICAS. **NBR 9778**: argamassa e concreto endurecidos: determinação da absorção de água, índice de vazios e massa específica. Rio de Janeiro, 2005a.

ASSOCIAÇÃO BRASILEIRA DE NORMAS TÉCNICAS. **NBR 9833**: concreto fresco: determinação da massa específica, do rendimento e do teor de ar pelo método gravimétrico. Rio de Janeiro, 2008.

BERNARDO, L. M. **Aplicação de concretos especiais com sílica coloidal como material de reparo de estruturas de concreto**. São Carlos, 2024. 112 f. Dissertação (Mestrado em Ciências – Engenharia Civil) – Escola de Engenharia de São Carlos, Universidade de São Paulo, São Carlos, 2024.

BJÖRNSTRÖM, J. *et al.* Accelerating effects of colloidal nano-silica for beneficial calcium-silicate-hydrate formation in cement. **Chemical Physics Letters**, v. 392, n. 1, p. 242-248, 2004.

DU, H. *et al.* Effect of nano-silica on mechanical and transport properties of lightweight concrete. **Construction and Building Materials**, v. 82, p. 114-122, 2015.

FAGURY, S.C. **Concretos e pastas de elevado desempenho: contribuição aos estudos de reparos estruturais e ligações entre concreto novo e velho, com tratamento da zona de interface**. São Carlos, 2002.184 f. Dissertação (Mestrado em Ciência e Engenharia de Materiais) – Escola de Engenharia de São Carlos, Universidade de São Paulo, São Carlos, 2002.

FUNK, J. E.; DINGER, D. R. **Predictive process control of crowded particulate suspensions**: applied to ceramic manufacturing. Nova York: Springer Science Business Media, 1994.

HELENE, P.; TERZIAN, P. Manual de dosagem e controle do concreto. São Paulo: PINI; Brasília: SENAI, 1992.

INTERNATIONAL ORGANIZATION FOR STANDARTIZATION. **ISO 13320**: particle size analysis: laser diffraction methods. Brussels, 2020.

JALAL, M. *et al.* Comparative study on effects of Class F fly ash, nano silica and silica fume on properties of high performance self-compacting concrete. **Construction and Building Materials**, v. 95, p. 366-374, 2015.

JO, B. W. *et al.* Investigations on the development of powder concrete with nano-SiO_2 particles. **KSCE Journal of Civil Engineering**, v. 11, p. 37-42, 2007.

KONG, D. *et al.* Effect and mechanism of colloidal silica sol on properties and microstructure of the hardened cement-based materials as compared to nano-silica powder with agglomerates in micron-scale. Cement and Concrete Composites, v. 98, p. 137-149, 2019.

LI, H. *et al*. Microstructure of cement mortar with nano-particles. **Composites Part B: Engineering**, v. 35, p. 185-189, 2004.

LI, L. G. *et al*. Synergistic effects of micro-silica and nano-silica on strength and microstructure of mortar. **Construction and Building Materials**, v. 140, p. 229-238, 2017.

LOPES, H. M. T. **Aplicação do conceito de empacotamento de partículas na otimização de dosagem de concretos de cimento Portland**. São Carlos, 2019. 174 f. Dissertação (Mestrado em Ciências – Engenharia Civil) – Escola de Engenharia de São Carlos, Universidade de São Paulo, São Carlos, 2019.

LTIFI, M. *et al*. Experimental study of the effect of addition of nano-silica on the behaviour of cement mortars. **Procedia Engineering**, v.10, p. 900-905, 2011.

MAGLIANO, M. V. M. **Sílica coloidal como agente ligante e fonte mulitizadora em concretos refratários**. São Carlos, 2009. 163 f. Dissertação (Mestrado em Engenharia de Materiais) – Universidade Federal de São Carlos, São Carlos, 2009.

MEDEIROS, A. G. *et al*. Aplicação de metodologias de inspeção em ponte de concreto armado. **Ambiente Construído**, Porto Alegre, v. 20, n. 3, p. 687-702, jul./set. 2020.

MEHTA, K.; MONTEIRO P. J. M. **Concreto**: microestrutura, propriedades e materiais. 4. ed. São Paulo: IBRACON, 2014.

NAIK, T. R.; MALHOTRA, V. M.; POPOVICS, J. S. The ultrasonic pulse velocity method. In: MALHOTRA, V. M.; CARINO, N. J. (ed.). **Handbook on nondestructive testing of concrete**. 2. ed. Boca Raton: CRC Press, 2004.

NORHASRI, M. S. M. *et al.* Applications of using nano material in concrete: a review. **Construction and Building Materials**, v. 133, p. 91-97, 2017.

OLIVEIRA, C. O. *et al.* Impacto do conceito de empacotamento de partículas na dosagem de concretos de alto desempenho. **Revista Matéria**, e-11962, 2018.

PRADO, L. P. **Estudo da interface do concreto pré-moldado e concreto de altíssimo desempenho reforçado com fibras**. São Carlos, 2020. 291 f. Tese (Doutorado em Ciências – Engenharia Civil) **-** Escola de Engenharia de São Carlos, Universidade de São Paulo, São Carlos, 2020.

QING, Y. *et al.* Influence of nano-SiO_2 addition on properties of hardened cement paste as compared with silica fume. **Construction and Building Materials**, v. 21. p. 539-545, 2007.

QUERCIA, G. *et al.* Water demand of amorphous nano silica and its impact on the workability of cement paste. **Cement and Concrete Research**, v. 42, p. 344-357, 2012.

RUPASINGHE, R. *et al.* Nanoengineering concrete for sustainable built environment: a review. In: INTERNATIONAL CONFERENCE ON STRUCTURAL ENGINEERING CONSTRUCTION AND MANAGEMENT, 2., Kandy, 2011. **Proceedings […]** Kandy, 2011.

SAID, A. M. *et al.* Properties of concrete incorporating nano-SiO_2. **Construction and Building Materials**, v. 36, p. 838-844, 2012.

SALEMI, N.; BEHFARNIA, N. Effect of nano-particles on durability of fiber reinforced concrete pavement. *Construction and Building Materials*, v. 48, p. 934-941, 2013.

SANTOS, M. O. **Estudos de concretos com adição de sílica coloidal submetidos à ação combinada de cloretos e CO_2**. São Carlos, 2019. 125 f. Dissertação (Mestrado em Estruturas e Construção Civil) – Universidade Federal de São Carlos, São Carlos, 2019.

SINGH, L. P. *et al.* Beneficial role of nanosilica in cement based materials: a review. **Construction and Building Materials**, v. 47, p. 1069-1077, 2013.

SUPIT, S. W. M.; SHAIKH, F. U. A. Durability properties of high volume fly ash concrete containing nano-silica. **Materials and Structures**, v. 48, p. 2431–2445, 2015.

VASKE, N. R. *et al.* Aplicação de argamassa com adição de sílica ativa como material de reforço em elementos comprimidos de concreto. **Ambiente Construído**, v. 8, n. 3, p. 77–93, jul./set. 2008.

YUN, K. *et al.* Influence of colloidal silica and silica fume on the rheology and mechanical properties of high-performance shotcrete. **KSCE Journal of Civil Engineering**, v. 26, p. 2737-2746, 2022.

ZHANG, P. *et al.* Mechanical properties of fly ash concrete composite reinforced with nano-SiO_2 and steel fiber. **Current Science**, v. 106, p. 1529-1537, 2014.

Acknowledgments

The authors would like to thank the Coordenação de Aperfeiçoamento de Pessoal de Nível Superior (CAPES) for financial support through a scholarship, the companies Chryso Saint-Gobain, Elkem and Nouryon for donating the materials used in the research, and the Departamento de Engenharia de Estruturas da Escola de

Engenharia de São Carlos da Universidade de São Paulo (SET/EESC/USP) for the infrastructure provided for the tests.

Declaration of Generative AI and AI-Assisted Technologies in the Writing Process
The present paper was prepared by the authors without the use of any generative AI tools.

Financial Support
This study was financed by the Coordenação de Aperfeiçoamento de Pessoal de Nível Superior (CAPES) – Finance Code 001.

Data Availability Statement
The data supporting the findings of this study are available from publicly accessible master's thesis, which served as the foundation for this research. It can be accessed at the following link: https://producaocientifica.eesc.usp.br/set/1320?search=modotte. Additional data generated or analysed in this study are available from the corresponding author on reasonable request.

Conflict of Interest
The authors have no competing interests to declare that might be relevant to the content of this paper.

Authors' Contribution
Lucas M. Bernardo: Funding acquisition; Conceptualization, Data curation, Formal analysis, Investigation, Methodology, Validation, Visualization, Writing – original draft. **Alessandra L. de Castro**: Conceptualization, Methodology, Supervision, Visualization, Writing – review & editing.

Editor-in-chief: **Marcelo Henrique Farias de Medeiros**

Ambiente Construído
Revista da Associação Nacional de Tecnologia do Ambiente Construído
Av. Osvaldo Aranha, 99 - 3º andar, Centro
Porto Alegre – RS - Brasil
CEP 90035-190
Telefone: +55 (51) 3308-4084
www.seer.ufrgs.br/ambienteconstruido
www.scielo.br/ac
E-mail: ambienteconstruido@ufrgs.br